$$\mathbf{J} \times B = \left[ \frac{A_1 \sigma_f B_0^2}{1 + (A_1 m)^2} \left( -\overline{U} + A_1 m \overline{V} \right), \ \frac{-A_1 \sigma_f B_0^2}{1 + (A_1 m)^2} \left( \overline{V} + A_1 m \overline{U} \right), \ 0 \right], \tag{4}$$

where Hall parameter m and  $A_1$  are defined below:

$$m = \frac{\sigma_f B_0}{e n_e}, \ A_1 = 1 + \frac{3(\frac{\sigma_p}{\sigma_f} - 1)\varphi}{(\frac{\sigma_p}{\sigma_f} + 2) - (\frac{\sigma_p}{\sigma_f} - 1)\varphi}.$$

The Ohmic heating in view of Eqs. (1)-(3) is

$$\frac{1}{\sigma_{eff}} \mathbf{J}. J = \frac{A_1 \sigma_f B_0^2}{1 + (A_1 m)^2} (\overline{U}^2 + \overline{V}^2).$$
 (5)

Flow within the channel is induced due to propagation of sinusoidal waves of wavelength  $\lambda$  along the channel walls with constant speed c. Mathematically the geometry of peristaltic walls is given as follows:

$$\overline{H}_{1}(\overline{X}, \ \overline{t}) = d_{1} + a_{1} \cos\left(\frac{2\pi}{\lambda}(\overline{X} - c\overline{t})\right),$$

$$\overline{H}_{2}(\overline{X}, \ \overline{t}) = -d_{2} - b_{1} \cos\left(\frac{2\pi}{\lambda}(\overline{X} - c\overline{t}) + \gamma\right),$$
(6)

in which  $\overline{H}_{1,\,2}$  designate the peristaltic walls in the positive and negative  $\overline{Y}$  directions respectively,  $a_1$ ,  $b_1$  the amplitudes of waves traveling along  $\overline{H}_{1,\,2}$  and  $\gamma$  the phase difference of two waves. Walls at  $\overline{H}_1$  and  $\overline{H}_2$  are maintained at constant temperature  $T_0$  and  $T_1(>T_0)$  respectively. We transform our problem from fixed frame to wave frame. Transformations between the laboratory and wave frames are

$$\overline{x} = \overline{X} - c\overline{t}, \ \overline{y} = \overline{Y}, \ \overline{u} = \overline{U} - c, \ \overline{v} = \overline{V}, \ \overline{p}(\overline{x}, \ \overline{y}) = \overline{P}(\overline{X}, \ \overline{Y}, \ \overline{t}),$$
 (7)

where  $(\overline{x}, \overline{y})$  are the coordinates in the wave frame,  $\overline{u}$ ,  $\overline{v}$  the velocity components in the wave frame,  $\overline{P}(\overline{X}, \overline{Y}, \overline{t})$  and  $\overline{p}(\overline{x}, \overline{y})$  the pressure in fixed and moving frames respectively,  $(\overline{X}, \overline{Y})$  and  $(\overline{U}, \overline{V})$  the coordinates and velocity components in fixed frame. In wave frame the continuity equation for present flow configuration can be represented by the following expression

$$\frac{\partial \overline{u}}{\partial \overline{x}} + \frac{\partial \overline{v}}{\partial \overline{y}} = 0. \tag{8}$$

Components of the momentum equation taking into account the mixed convection and Lorentz force are

$$\begin{split} &((1-\varphi)\rho_{f}+\varphi\rho_{p})\bigg((\overline{u}+c)\frac{\partial}{\partial\overline{x}}+\overline{v}\frac{\partial}{\partial\overline{y}}\bigg)(\overline{u}+c)\\ &=-\frac{\partial\overline{p}}{\partial\overline{x}}-\frac{A_{1}\sigma_{f}B_{0}^{2}}{1+(A_{1}m)^{2}}((\overline{u}+c)-A_{1}m\overline{v})\\ &+\frac{\mu_{f}}{(1-\varphi)^{2.5}}\bigg(\frac{\partial^{2}\overline{u}}{\partial\overline{x}^{2}}+\frac{\partial^{2}\overline{u}}{\partial\overline{y}^{2}}\bigg)+g\bigg((1-\varphi)\rho_{f}\beta_{f}+\varphi\beta_{p}\rho_{p}\bigg)(T-T_{m}), \end{split} \tag{9}$$

$$((1 - \varphi)\rho_f + \varphi \rho_p) \left( (\overline{u} + c) \frac{\partial}{\partial \overline{x}} + \overline{v} \frac{\partial}{\partial \overline{y}} \right) \overline{v} = -\frac{\partial \overline{p}}{\partial \overline{y}}$$

$$+ \frac{\mu_f}{(1 - \varphi)^{2.5}} \left( \frac{\partial^2 \overline{v}}{\partial \overline{x}^2} + \frac{\partial^2 \overline{v}}{\partial \overline{y}^2} \right) - \frac{A_1 \sigma_f B_0^2}{1 + (A_1 m)^2} (\overline{v} + A_1 m(\overline{u} + c)).$$

$$(10)$$

The energy equation with the viscous dissipation, heat generation/absorption and Ohmic heating can be put into the following form:

$$((1 - \varphi)(\rho C)_{f} + \varphi(\rho C)_{p}) \left( (\overline{u} + c) \frac{\partial}{\partial \overline{x}} + \overline{v} \frac{\partial}{\partial \overline{y}} \right) T$$

$$= K_{eff} \left( \frac{\partial^{2} T}{\partial \overline{x}^{2}} + \frac{\partial^{2} T}{\partial \overline{y}^{2}} \right) + \Phi$$

$$+ \frac{\mu_{f}}{(1 - \varphi)^{2.5}} \left[ 2 \left( \left( \frac{\partial \overline{u}}{\partial \overline{x}} \right)^{2} + \left( \frac{\partial \overline{v}}{\partial \overline{y}} \right)^{2} \right) + \left( \frac{\partial \overline{u}}{\partial \overline{y}} + \frac{\partial \overline{v}}{\partial \overline{x}} \right)^{2} \right]$$

$$+ \frac{A_{1} \sigma_{f} B_{0}^{2}}{1 + (A_{1} m)^{2}} \left( (\overline{u} + c)^{2} + \overline{v}^{2} \right). \tag{11}$$

In the formulation of above equations we have used the two phase flow model with values of effective density  $\rho_{eff}$ , specific heat  $C_{eff}$  and thermal conductivity  $K_{eff}$  as follows [10,11,28,29]:

$$\rho_{eff} = (1 - \varphi)\rho_{f} + \varphi\rho_{p}, 
(\rho C)_{nf} = (1 - \varphi)(\rho C)_{f} + \varphi(\rho C)_{p}, 
(\rho \beta)_{nf} = (1 - \varphi)\rho_{f}\beta_{f} + \varphi\rho_{p}\beta_{p}, 
\frac{K_{eff}}{K_{f}} = \frac{K_{p} + 2K_{f} - 2\varphi(K_{f} - K_{p})}{K_{p} + 2K_{f} + \varphi(K_{f} - K_{p})}.$$
(12)

here  $\mu_f$  is the viscosity of water, g the acceleration due to gravity,  $\beta_f$  the thermal expansion coefficient of water,  $\beta_p$  the thermal expansion coefficient of copper nanoparticles, T the temperature of nanofluid,  $T_m \left( = \frac{T_1 + T_0}{2} \right)$  the mean temperature,  $C_f$  the specific heat of water,  $C_p$  the specific heat of the copper

**Table 1**Numerical values of thermo-physical properties of water and copper.

Phase	ρ (kg/m3)	K (W/mK)	C (J/kgK)	$\beta \left( 1/k\right) \times 10^{-6}$	σ (S/m)
Water	997.1	0.613	4179	210	$0.05 \\ 5.96 \times 10^7$
Copper (Cu)	8933	401	385	16.65	

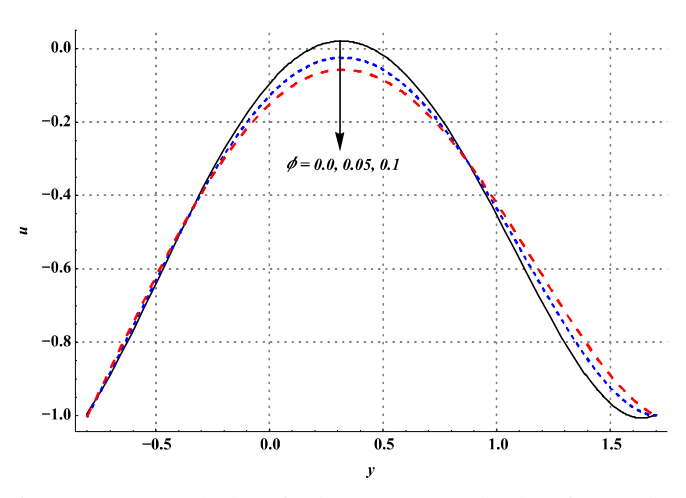


**Fig. 1.** Variation in axial velocity for change in nanoparticle volume fraction when Gr=3.0, a=0.7, b=0.6,  $\gamma=\pi/2$ , d=0.8, x=1,  $\eta=0.7$ , M=1.0, m=2, Br=0.3 and  $\varepsilon=2.5$ .

nanoparticles,  $\Phi$  the dimensional heat generation/absorption [28,29],  $K_f$  the thermal conductivity of water and  $K_p$  the thermal conductivity of copper nanoparticles. Values of the thermo-physical properties of water and copper are given through Table 1 [10,28,29].

The long wave length and low Reynolds number approximation are extensively used in the analysis of peristaltic flows [24–27]. The long wavelength approximation is based on the assumption that wavelength of the peristaltic wave is considerably large when compared with the half width of the channel/tube. The Reynolds number is also assumed small. These considerations are relevant for the case of chyme transport through small intestine [12] where  $d_1 = 1.25$  cm and  $\lambda = 8.01$  cm. Clearly half width of the intestine is small in comparison to the wavelength of peristaltic wave i.e.  $a_1/\lambda = 0.156$ . Further, Lew et al. [13] concluded that Reynolds number for the fluid mechanics in small intestine is small. Making use of the following dimensionless quantities

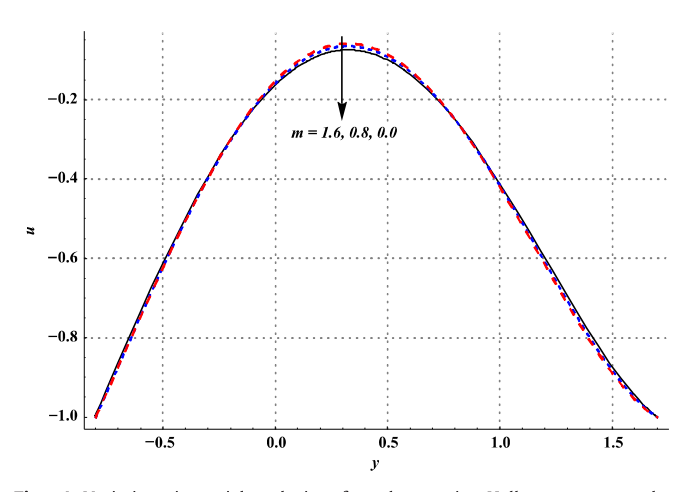


**Fig. 4.** Variation in axial velocity for change in Hall parameter when  $Gr=3.0,\ a=0.7,\ b=0.6,\ \gamma=\pi/2,\ d=0.8,\ x=1,\ \eta=0.7,\ M=1.0,\ \varphi=0.1,\ Br=0.3$  and  $\varepsilon=2.5.$ 

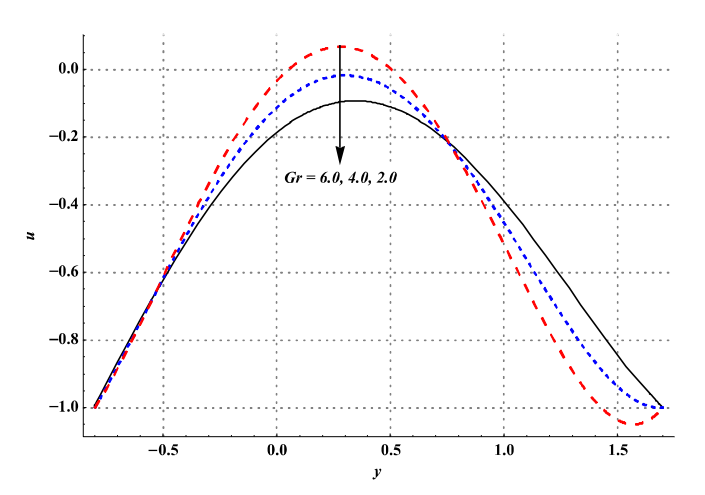


**Fig. 2.** Variation in axial velocity for change in Grashoff number when  $\varphi=0.1,~a=0.7,~b=0.6,~\gamma=\pi/2,~d=0.8,~x=1,~\eta=0.7,~M=1.0,~m=2,~Br=0.3$  and  $\varepsilon=2.5.$ 

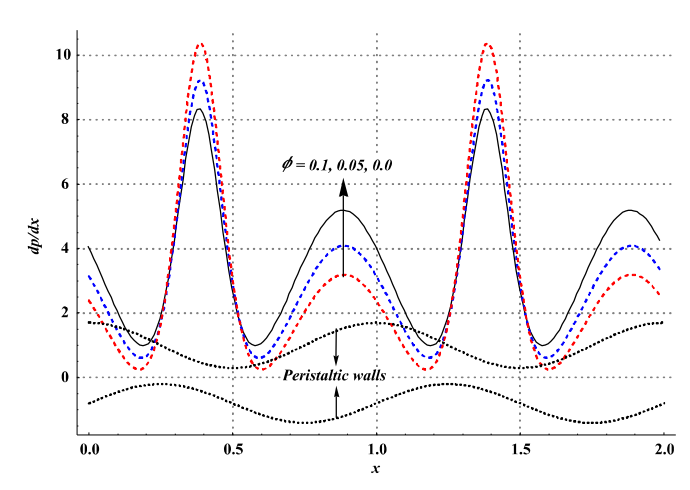


**Fig. 5.** Impact of nanoparticle volume fraction on pressure gradient when Gr = 3.0, a = 0.7, b = 0.6,  $\gamma = \pi/2$ , d = 0.8,  $\eta = 0.5$ , M = 1.0, m = 2, Br = 0.3 and  $\varepsilon = 2.5$ .

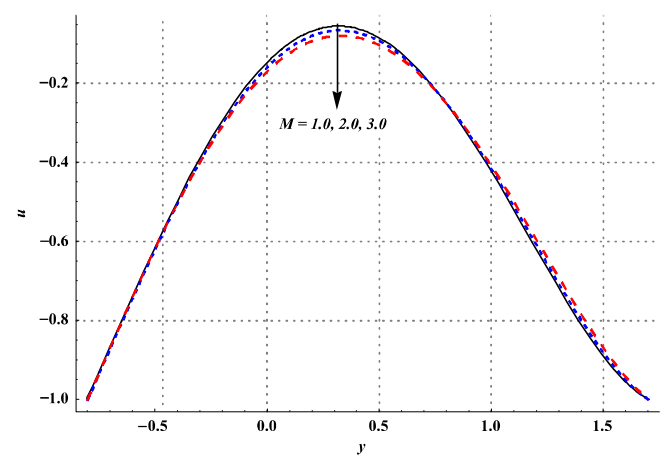


**Fig. 3.** Variation in axial velocity for change in Hartman number when Gr=3.0, a=0.7, b=0.6,  $\gamma=\pi/2$ , d=0.8, x=1,  $\eta=0.7$ ,  $\varphi=0.1$ , m=2, Br=0.3 and  $\varepsilon=2.5$ .

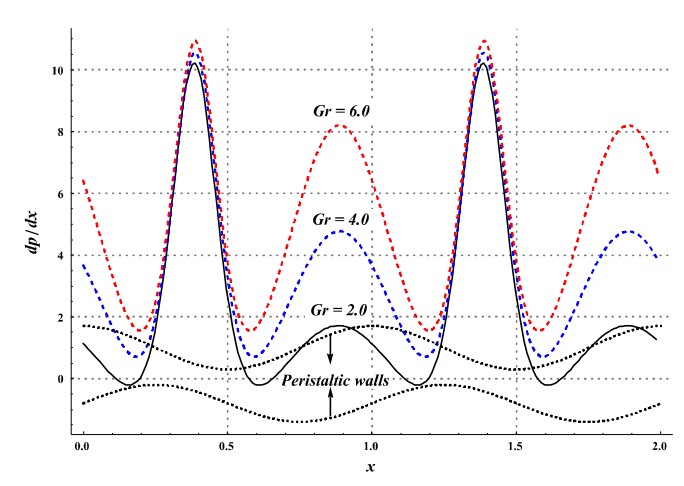


**Fig. 6.** Impact of Grashoff number on pressure gradient when  $\varphi=0.1$ , a=0.7, b=0.6,  $\gamma=\pi/2$ , d=0.8,  $\eta=0.5$ , M=1.0, m=2, Br=0.3 and  $\varepsilon=2.5$ .

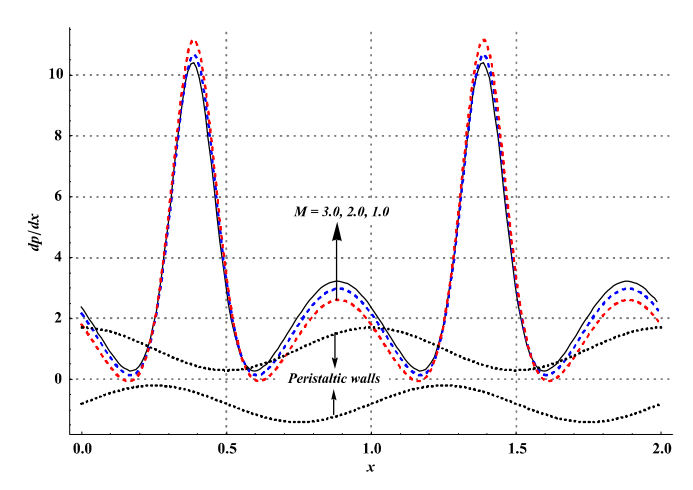


**Fig. 7.** Impact of Hartman number on pressure gradient when  $Gr=3.0,\ a=0.7,\ b=0.6,\ \gamma=\pi/2,\ d=0.8,\ \eta=0.5,\ \varphi=0.1,\ m=2,\ Br=0.3$  and  $\varepsilon=2.5.$ 

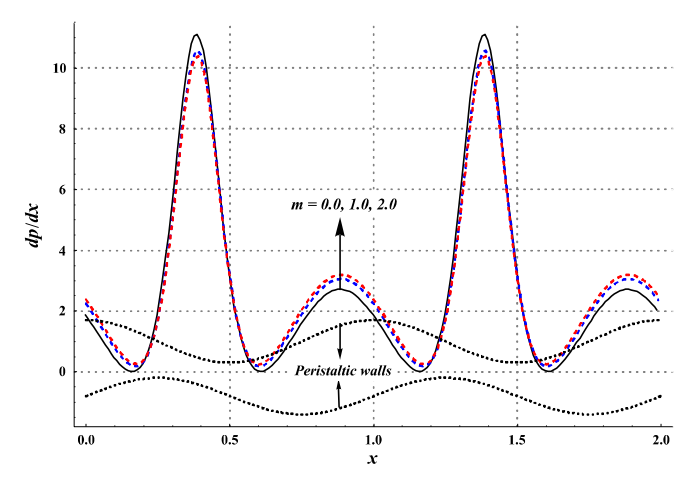


**Fig. 8.** Impact of Hall parameter on pressure gradient when Gr=3.0, a=0.7, b=0.6,  $\gamma=\pi/2$ , d=0.8,  $\eta=0.5$ ,  $\varphi=0.1$ ,  $\varphi=0.1$ , Br=0.3 and  $\varepsilon=2.5$ .

$$x = \frac{\overline{x}}{\lambda}, \quad y = \frac{\overline{y}}{d_1}, \quad i = \frac{\overline{u}}{c}, \quad v = \frac{\overline{v}}{c\delta},$$

$$\delta = \frac{d_1}{\lambda}, \quad h_1 = \frac{\overline{H}_1}{d_1}, \quad h_2 = \frac{\overline{H}_2}{d_1},$$

$$d = \frac{d_2}{d_1}, \quad a = \frac{a_1}{d_1}, \quad b = \frac{b_1}{d_1}, \quad p = \frac{d_1^2 \overline{p}}{c\lambda \mu_f}, \quad \text{Re} = \frac{\rho_f c d_1}{\mu_f}, \quad M = \sqrt{\frac{\sigma_f}{\mu_f}} B_0 d_1,$$

$$Gr = \frac{\rho_f g \beta_f (T_1 - T_0) d_1^2}{\mu_f c}, \quad \theta = \frac{T - T_m}{T_1 - T_0}, \quad E = \frac{c^2}{C_f (T_1 - T_0)}, \quad \text{Pr} = \frac{\mu_f C_f}{K_f},$$

$$Br = \text{Pr} E, \quad \varepsilon = \frac{d_1^2 \Phi}{(T_1 - T_0) K_f}, \quad u = \frac{\partial \psi}{\partial y}, \quad v = -\frac{\partial \psi}{\partial x},$$

$$(13)$$

and adopting the long wavelength and small Reynolds number assumptions, Eqs. (9)-(11) are finally reduced in the following fashion:

$$\frac{\partial p}{\partial x} = \frac{1}{(1-\varphi)^{2.5}} \frac{\partial^3 \psi}{\partial y^3} + A_2 Gr\theta - \frac{A_1 M^2}{1 + (A_1 m)^2} \left(\frac{\partial \psi}{\partial y} + 1\right),\tag{14}$$

$$\frac{\partial p}{\partial y} = 0,\tag{15}$$

$$A_3 \frac{\partial^2 \theta}{\partial y^2} + \frac{Br}{(1 - \varphi)^{2.5}} \left( \frac{\partial^2 \psi}{\partial y^2} \right)^2 + \frac{BrA_1 M^2}{1 + (A_1 m)^2} (\frac{\partial \psi}{\partial y} + 1)^2 + \varepsilon = 0.$$
 (16)

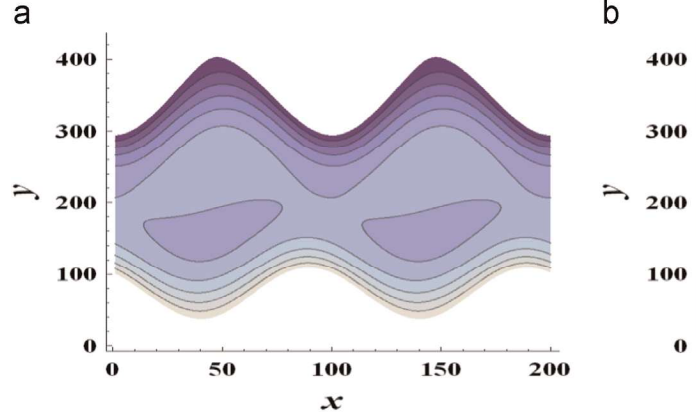
Eq. (15) shows that  $p \neq p(y)$  and by cross differentiation of Eqs. (14) and (15) one has

$$\frac{1}{(1-\varphi)^{2.5}} \frac{\partial^4 \psi}{\partial y^4} + A_2 Gr \frac{\partial^2 \theta}{\partial y^2} - \frac{A_1 M^2}{1 + (A_1 m)^2} \frac{\partial^2 \psi}{\partial y^2} = 0.$$
 (17)

here  $\delta$  is the wave number,  $h_{1,2}$  the dimensionless walls, d the channel width ratio, a, b the dimensionless amplitudes, p the dimensionless pressure, Re the Reynolds number, M the Hartman number, Gr the Grashoff number,  $\theta$  the dimensionless temperature, E the Eckert number, Pr the Prandtl number, E the Brinkman number, E the dimensionless heat generation/absorption parameter and E0 the stream function. Further the continuity equation is identically satisfied and E1, appearing in these equations are given below:

$$A_{2} = \left\{ 1 - \varphi + \varphi \left( \frac{(\rho \beta)_{p}}{(\rho \beta)_{f}} \right) \right\}, \ A_{3} = \frac{K_{p} + 2K_{f} - 2\varphi(K_{f} - K_{p})}{K_{p} + 2K_{f} + \varphi(K_{f} - K_{p})}.$$
(18)

Dimensionless mean flow rates in the laboratory  $\eta(=\frac{\overline{Q}}{cd_1})$  and wave frames  $F(=\frac{\overline{q}}{cd_1})$  are related by



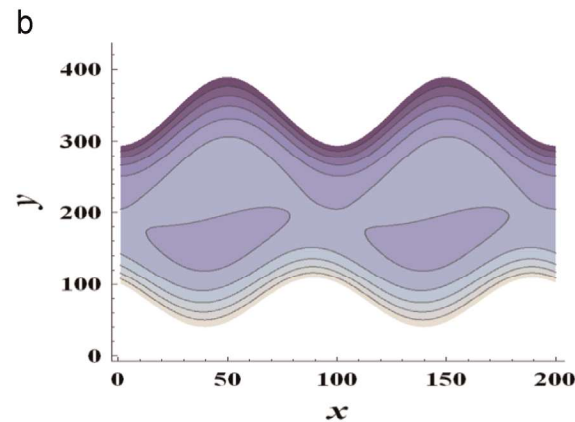


**Fig. 9.** (a and b). Streamlines for variation in the value of nanoparticle volume fraction when Gr = 2.0, a = 0.4, b = 0.3,  $\gamma = \pi/2$ , d = 0.7,  $\eta = 1.3$ , M = 1.0, m = 2.0, Br = 0.3 and  $\varepsilon = 2.5$ . (a)  $\varphi = 0.0$  and (b)  $\varphi = 0.1$ .

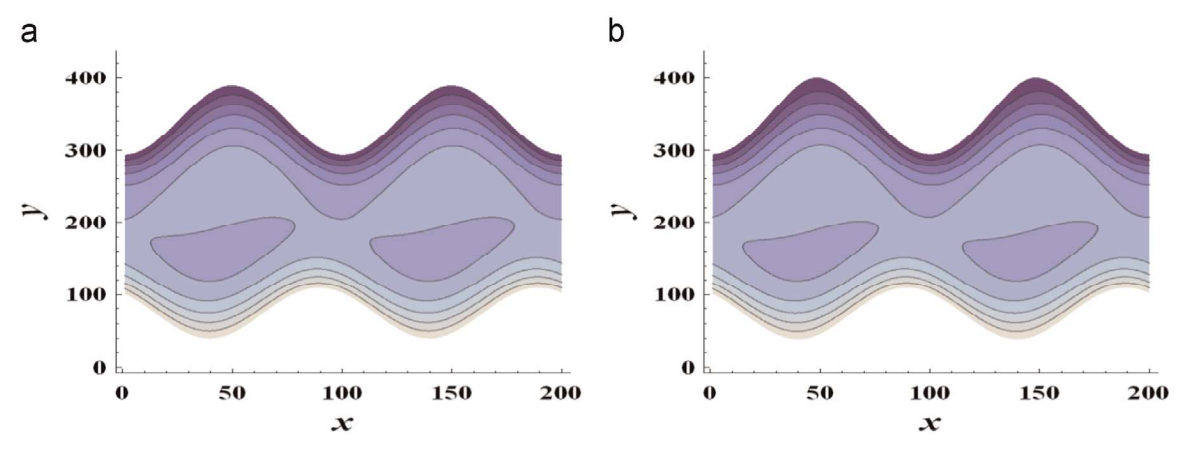


**Fig. 10.** (a and b). Streamlines for variation in the value of Grashoff number when  $\varphi = 0.1$ , a = 0.4, b = 0.3,  $\gamma = \pi/2$ , d = 0.7,  $\eta = 1.3$ , M = 1.0, m = 2.0, Br = 0.3 and  $\varepsilon = 2.5$ . (a) Gr = 2.0 and (b) Gr = 3.0.

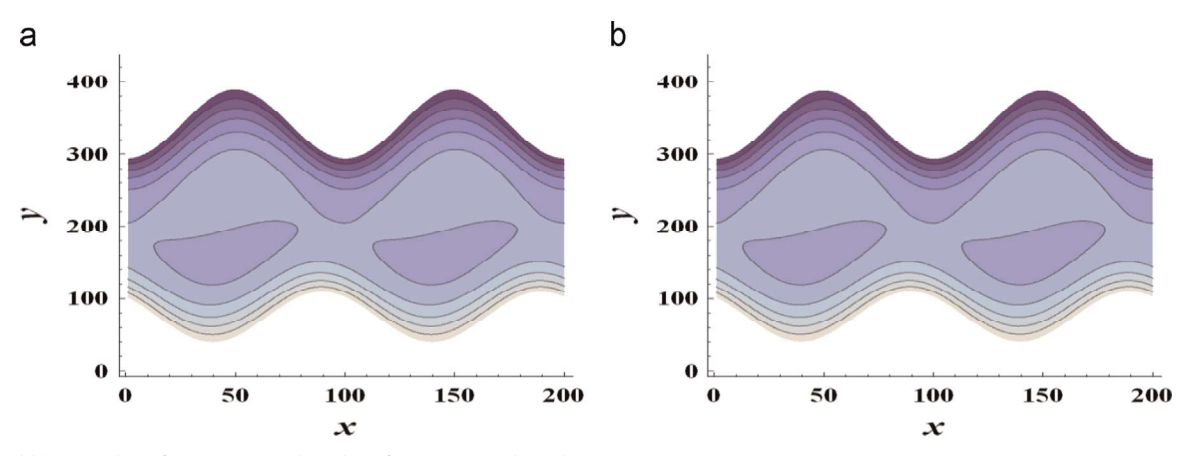


**Fig. 11.** (a and b). Streamlines for variation in the value of Hartman number when  $\varphi = 0.1$ , a = 0.4, b = 0.3,  $\gamma = \pi/2$ , d = 0.7,  $\eta = 1.3$ , Gr = 2.0, m = 2.0, Br = 0.3 and  $\varepsilon = 2.5$ . (a) M = 1.0 and (b) M = 2.0.

$$\eta = F + 1 + d,\tag{19}$$

where  $\overline{Q}$ ,  $\overline{q}$  are the dimensional mean flow rates in the laboratory and wave frames and

$$F = \int_{h_2}^{h_1} \frac{\vartheta \psi}{\vartheta \psi} dy. \tag{20}$$

The dimensionless boundary conditions are presented in the forms

$$\psi = \frac{F}{2}, \frac{\partial \psi}{\partial y} = -1, \ \theta = -\frac{1}{2}, \text{ at } y = h_1,$$

$$\psi = -\frac{F}{2}, \frac{\partial \psi}{\partial y} = -1, \ \theta = \frac{1}{2}, \text{ at } y = h_2.$$
(21)

Here  $h_1 = 1 + a\cos(2\pi x)$  and  $h_2 = -d - b\cos(2\pi x + \gamma)$  are the dimensionless wall shapes of the peristaltic walls. The system of Eqs. (13)–(15) subject to boundary conditions (20) is solved numerically using NDSolve in **Mathematica**. Graphical analysis of the numerical data is presented in the next section.

## 3. Discussion

Effects of embedded parameters on the quantities of interest are examined through plots in this section. Plots for the axial velocity, pressure gradient, streamlines, temperature and heat transfer rate at the wall are obtained and studied through Figs. 1–19. Comparison of the influence of applied magnetic field on the

velocity and temperature in presence and absence of Hall effects is given through Table 2. For the sake of better representation we divide this section into two subsection namely (a) flow behavior analysis and (b) heat transfer analysis.

## 3.1. Flow behavior analysis

Plots of velocity profile for variation in nanoparticle volume fraction, Grashoff number, Hartman number and Hall parameter are shown in the Figs. 1-4. These Figs. witness that the plots for velocity are concaved downward. These plots show a parabolic trajectory with maximum value occurring near the center of channel. Water free of nanoparticles has higher velocity near the center of channel (see Fig. 1). This figure also shows that an increase in the nanoparticle volume fraction further reduces the maximum value of velocity. Primarily this is because of the fact that addition of nanoparticles increases the resistance to the flow due to higher density of nanoparticles. In a two phase flow model (as used in this study) the effective viscosity of the nanofluid enhances by increasing the nanoparticle volume fraction which provides higher resistance to the fluid motion. Fig. 2 is prepared to note the effect of Grashoff number on the fluid velocity. This figure indicates that higher values of the fluid velocity near the center are achieved in mixed convective flows. Physically this indicates that density variations due to temperature difference facilitate the fluid's motion. Hartman number and Hall parameter have opposite effects on the velocity of nanofluid (see Figs. 3 and 4). Increase in the value of Hartman number results in a decrease of the velocity

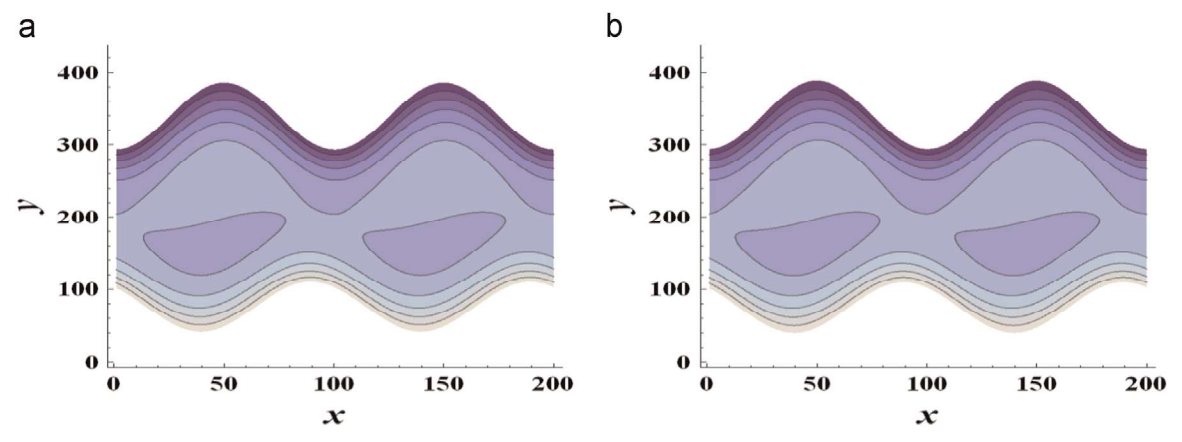


**Fig. 12.** (a and b). Streamlines for variation in the value of Hall when  $\varphi = 0.1$ , a = 0.4, b = 0.3,  $\gamma = \pi/2$ , d = 0.7,  $\eta = 1.3$ , M = 1.0, Gr = 2.0, Br = 0.3 and  $\varepsilon = 2.5$ . (a) m = 0.0 and (b) m = 2.0.

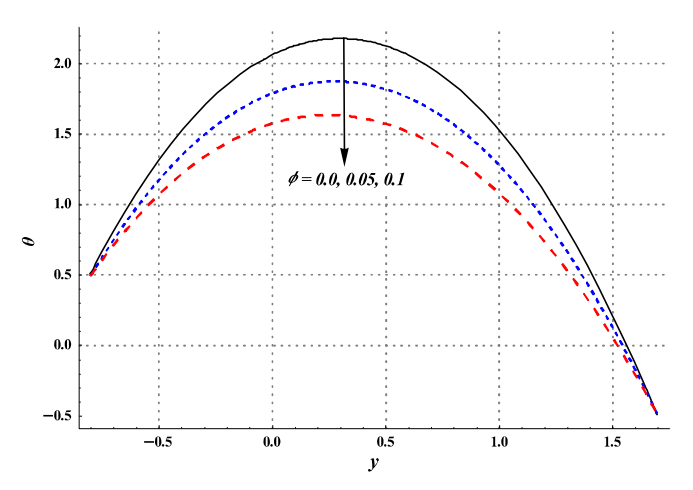


**Fig. 13.** Variation temperature for change in nanoparticle volume fraction when  $Gr=3.0,\ a=0.7,\ b=0.6,\ \gamma=\pi/2,\ d=0.8,\ x=1,\ \eta=0.7,\ M=1.0,\ m=2.0,\ Br=0.3$  and  $\varepsilon=2.5.$ 

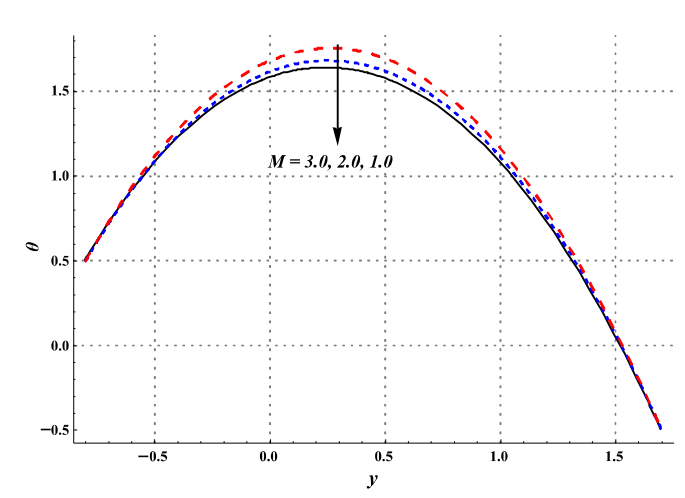


**Fig. 15.** Variation temperature for change in Hartman when Gr = 3.0, a = 0.7, b = 0.6, γ = π/2, d = 0.8, x = 1, η = 0.7, φ = 0.1, m = 2.0, Br = 0.3 and ε = 2.5.

= 0.0, 0.8, 1.6

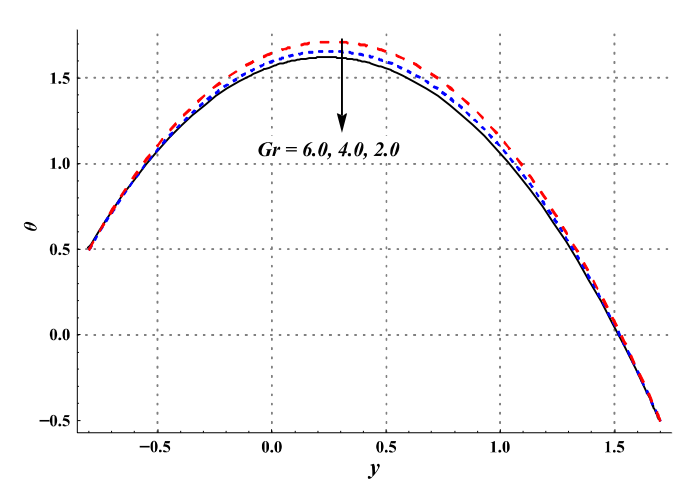
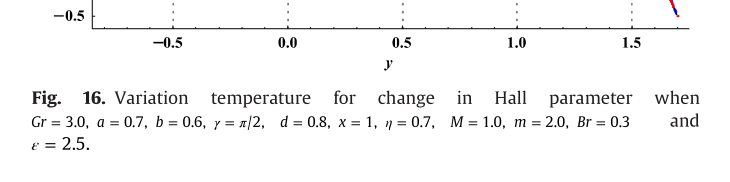


**Fig. 14.** Variation temperature for change in Grashoff number when  $\varphi=0.1,\ a=0.7,\ b=0.6,\ \gamma=\pi/2,\ d=0.8,\ x=1,\ \eta=0.7,\ M=1.0,\ m=2.0,\ Br=0.3$  and  $\varepsilon=2.5.$ 



near the center indicating the resistive nature of the Lorentz force. Hall effects on the other hand resist the changes brought by the rise in Hartman number. From Table 3 it can be seen that

maximum value of the velocity decreases rapidly with an increase in Hartman number when the Hall effects are absent. More controlled decrease in the velocity is noted for rise in Hartman number when Hall effects are taken into consideration (see